Nanoscale Res Lett (2008) 3:496–501
DOI 10.1007/s11671-008-9186-5

NANO EXPRESS

Synthesis of Organic Dye-Impregnated Silica Shell-Coated Iron Oxide Nanoparticles by a New Method

Cuiling Ren · Jinhua Li · Qian Liu · Juan Ren · Xingguo Chen · Zhide Hu · Desheng Xue

Received: 26 August 2008 / Accepted: 3 October 2008 / Published online: 23 October 2008

Abstract A new method for preparing magnetic iron oxide nanoparticles coated by organic dye-doped silica shell was developed in this article. Iron oxide nanoparticles were first coated with dye-impregnated silica shell by the hydrolysis of hexadecyltrimethoxysilane (HTMOS) which produced a hydrophobic core for the entrapment of organic dye molecules. Then, the particles were coated with a hydrophilic shell by the hydrolysis of tetraethylorthosilicate (TEOS), which enabled water dispersal of the resulting nanoparticles. The final product was characterized by X-ray diffraction, transmission electron microscopy, Fourier transform infrared spectroscopy, photoluminescence spectroscopy, and vibration sample magnetometer. All the characterization results proved the final samples possessed magnetic and fluorescent properties simultaneously. And this new multifunctional nanomaterial possessed high photostability and minimal dye leakage.

Keywords Fluorescent · Magnetic · Nanostructure · Synthesis · Hydrophobic silane

Introduction

Recently, fluorescent-magnetic bifunctional nanomaterials which are composed of magnetic iron oxide nanoparticles and luminescent dye-doped silica matrix gained more and more attention [1–10]. On the one hand, superparamagnetic iron oxide nanoparticles including maghemite (γ-Fe_2O_3) and magnetite (Fe_3O_4) were widely investigated for in vivo and in vitro biomedical applications, such as magnetic resonance imaging (MRI), target drug delivery, and so on [11–14]. On the other hand, dye-doped silica nanoparticles were good candidate for bio-labeling and bio-imaging because they showed several advantages, including photostable, sensitive, water soluble, and easy surface modification [15–17]. So these bi-functional nanoparticles could provide fluorescent and magnetic properties simultaneously which make them useful in highly efficient human stem cell labeling, magnetic carrier for photodynamic therapy, and other biomedical applications [1–3, 5–8].

Up to now, several methods have been developed for preparing such fluorescent-magnetic bi-functional nanomaterials [2–5]. Lee et al. have conjugated dye-doped silica with iron oxide nanoparticles by surface modification method [2]. Alternatively, organic dye-incorporated silica shell-coated iron oxide nanoparticles can be prepared in a reverse micelle system [3, 4]. These strategies could produce high quality fluorescent-magnetic nanoparticles, but they either needed expensive reagents or complicated synthetic steps. Recently, Ma et al. have prepared inorganic dye-doped silica shell-coated iron oxide nanospheres by Stöber method which needed fewer organic solvents and the preparation procedure was convenient [5]. But compared with inorganic dye, organic dye molecules seem to be better option for bio-labeling and bio-analysis because of their relatively high intrinsic quantum yield. However, organic dye molecules are not easily doped in a silica matrix [18]. So, simple and economic method for preparing organic dye-impregnated silica shell-coated iron oxide nanoparticles is still needed to be developed.

C. Ren · J. Li · Q. Liu · J. Ren · X. Chen (✉) · Z. Hu
Department of Chemistry, Lanzhou University,
Lanzhou 730000, People's Republic of China
e-mail: chenxg@lzu.edu.cn

D. Xue
Key Laboratory for Magnetism and Magnetic Materials of MOE,
Lanzhou University, Lanzhou 730000,
People's Republic of China

Recent studies indicated that hydrophobic silane was a good candidate to entrap organic dye into the silica matrix [18, 19]. So we developed a new method for preparing organic dye-impregnated silica shell-coated iron oxide nanoparticles based on the hydrolysis of HTMOS and TEOS. Iron oxide nanoparticles were first coated with a dye-impregnated silica shell by the hydrolysis of HTMOS which produced a hydrophobic environment for entrapping organic dye molecules (Rhodamine 6G was used as model dye). Subsequently, the particles were coated with a hydrophilic shell by the hydrolysis of TEOS, which enabled the resulting nanoparticles to be dispersed in aqueous solution. Herein, the synthesis procedure and the characterizations of the final multifunctional nanomaterial were summarized in detail.

Experimental Section

Chemical Reagents

Rhodamine 6G was commercially available from Dongsheng chemical reagent company, China. Hexadecyltrimethoxysilane (HTMOS) was purchased from Fluka chemical company. Tetraethylorthosilicate (TEOS) was purchased from Tianjin chemical reagent company, China. $NH_3 \cdot H_2O$ was a product of Baiyin chemical reagent company, China. All chemicals were used as received without further purification. Distilled water was used through the experiment.

Chemical Procedure

Iron oxide nanoparticles were prepared by adding ammonia to an aqueous solution of Fe^{2+}/Fe^{3+} at a 1:2 molar ratio [10]. The final product was denoted as S_1.

Then the iron oxide nanoparticles were coated with Rhodamine 6G doped silica shell. Typically, 0.75 mL of S1, 1.5 mL of H_2O, 0.6 mL of ammonia, and 10 mL of isopropyl alcohol were mixed together under magnetic stirring. Subsequently, 5 mL of Rhodamine 6G solution in isopropyl alcohol and appropriate volume of HTMOS was added into the mixture. After stirring for 3.0 h, 5 mL of isopropyl alcohol and 80 μL of TEOS were added into the reaction mixture. Two hours later, the formed product was centrifuged and washed with ethanol to remove the unreacted Rhodamine 6G and silane. The final particles were denoted as FS6 nanoparticles.

For comparison, Rhodamine 6G-doped silica shell-coated iron oxide nanoparticles were also prepared according to Ma's report with some modification [5]. Typically, 0.75 mL of S1, 1.75 mL of H_2O, 0.4 mL of ammonia, 12.5 mL of isopropyl alcohol, and 10 μL TEOS were mixed together. Then it was stirred for 3 h. Subsequently, 5 mL of Rhodamine 6G solution in isopropyl alcohol and 20 μL of TEOS were added into the mixture. After stirring for 0.5 h, 5 mL of isopropyl alcohol, 2.5 mL of H_2O, and 0.25 mL of ammonia was added dropwise into the reaction mixture simultaneously. The reaction mixture was further stirred for 24 h. The final product was denoted as FS62 nanoparticles.

Characterization

X-ray diffraction (XRD) pattern of the synthesized products were measured on an X' Pertpro Philips X-ray diffractometer from 10° to 90°. Transmission electron microscopy (TEM) was performed on a Hitachi-600 transmission electron microscope. A Nicolet Nexus 670 Fourier transform infrared spectra (FT-IR) spectrometer was employed to determine the chemical composition of the synthesized composites in the range of 4000–400 cm^{-1}. Magnetic property of the final sample was measured at room temperature by a vibration sample magnetometer (VSM, Lakeshore 730, America). A RF-5301 PC fluorescence spectrophotometer was used to determine the photoluminescence (PL) spectra of this multifunctional nanomaterial.

Results and Discussion

XRD spectrum of the FS6 nanoparticles is depicted in Fig. 1. The peaks in the range between 30° and 70° indicated the prepared iron oxide nanocrystals have an inverse spinel structure [20]. And their average particle size was calculated to be about 10 nm by (3 1 1) peak [21]. The broad featureless peak, which was found at the low

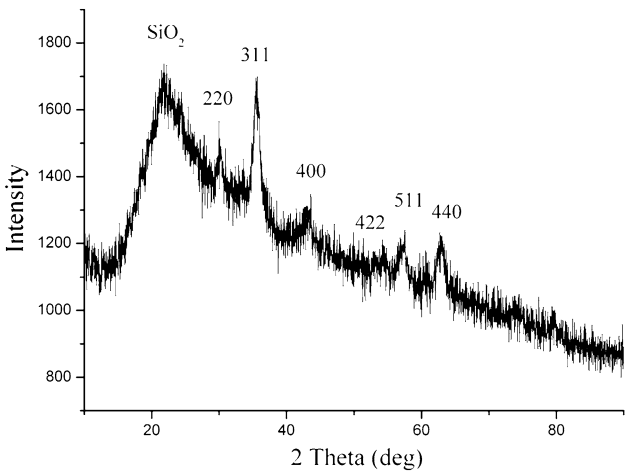

Fig. 1 XRD pattern of the FS6 nanoparticles

diffraction angle in Fig. 1, corresponds to the amorphous SiO_2 shell.

Figure 2 shows the representative TEM images of iron oxide nanoparticles and FS6 nanoparticles prepared under different conditions. As shown in Fig. 2a, the majority of the iron oxide nanoparticles were spherical with an average particle size around 10 nm, which was in agreement with the XRD result. As shown in Fig. 2b and c, with the other preparation conditions remaining the same, the average particle size of the FS6 nanoparticles prepared by 10 and 40 μL HTMOS correspond to 100 and 150 nm, respectively. It indicated the thickness of the silica shell could be tuned by simply varying the initial amount of HTMOS. But the silica shell was not very dense which may due to the long hydrophobic tail of HTMOS molecules. It was also found that water volume play an important role in controlling the morphology of the final particles. The volume of water used to prepare the particles in Fig. 2c and d was 1.5 and 0.75 mL, respectively. We can see that the final FS6 nanoparticles were all rather monodispersed, but the particles in Fig. 2d aggregated seriously. This observation suggested that the particles tended to aggregate as the volume of water decreased. Figure 2 demonstrates the magnetic nanoparticles have been entrapped in silica sphere successfully. But Rhodamine 6G could not be tested by TEM because it was molecule. So other measurements were still needed to prove the existence of Rhodamine 6G in the FS6 nanoparticles.

Figure 3 gives the FT-IR spectra of neat Rhodamine 6G, silica-coated magnetic particles (denoted as FS nanoparticles), and FS6 nanoparticles. The absorption bands for neat Rhodamine 6G [22] and FS nanoparticles [10] could be

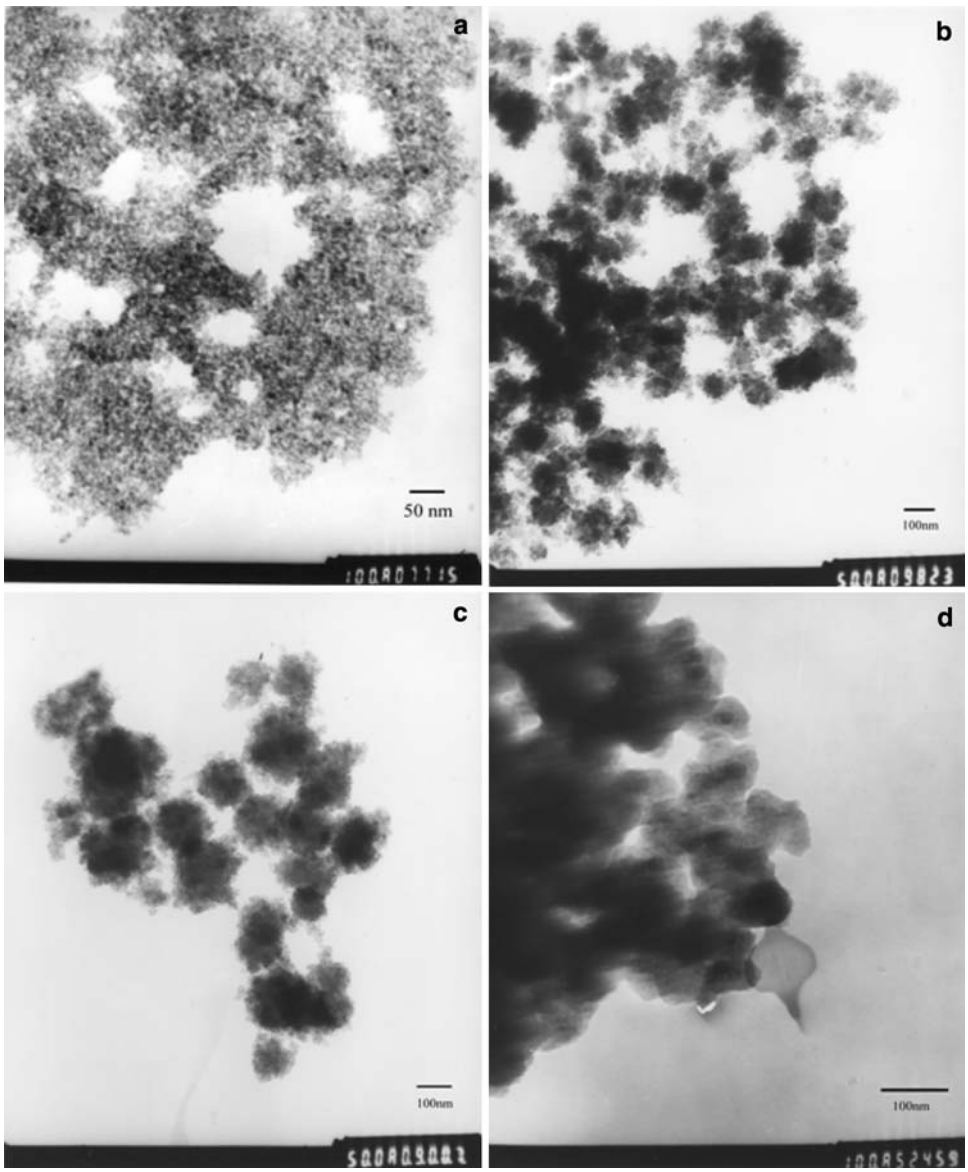

Fig. 2 TEM images for **a** iron oxide nanoparticles, **b** FS6 particles prepared by 10 μL HTMOS and 1.5 mL H_2O, **c** FS6 prepared by particles 40 μL HTMOS and 1.5 mL H_2O, **d** FS6 particles prepared by 40 μL HTMOS and 0.75 mL H_2O

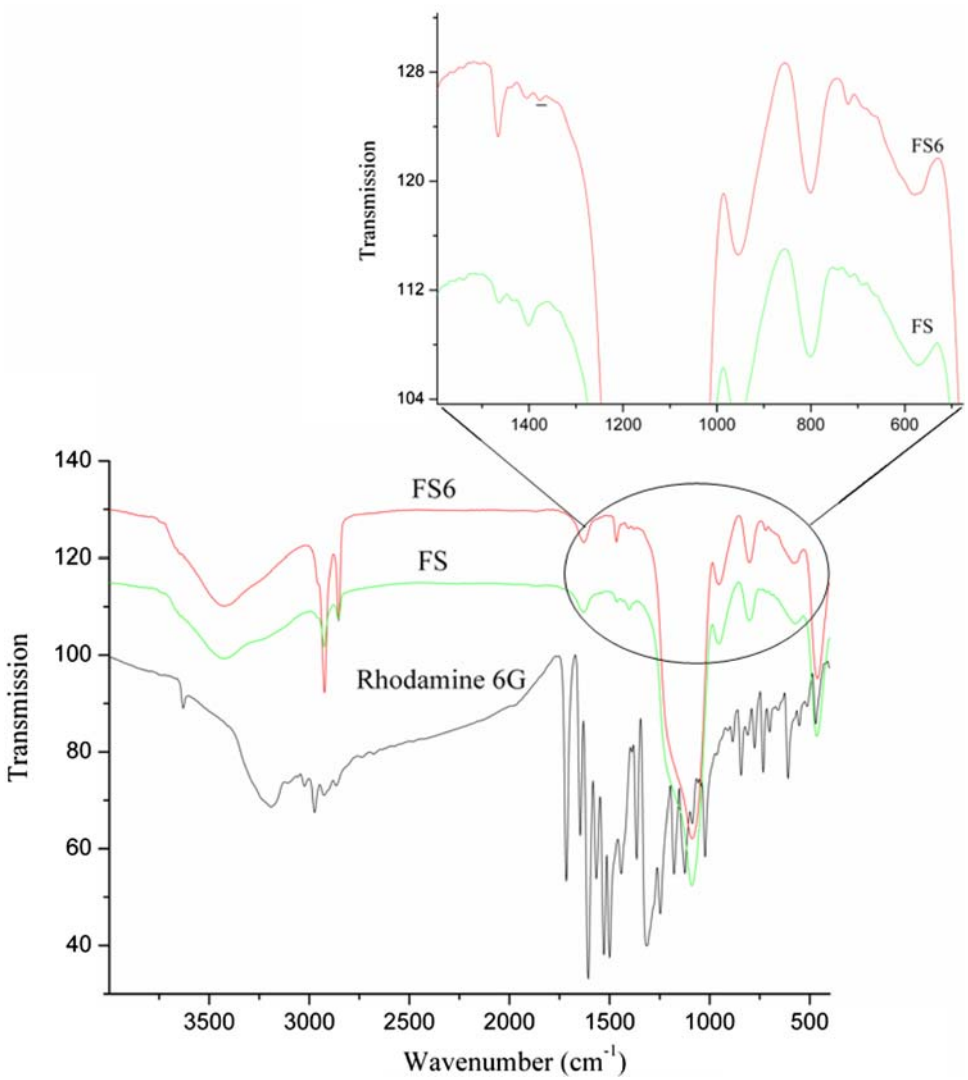

Fig. 3 FT-IR spectra of neat Rhodamine 6G, FS, and FS6 nanoparticles

well resolved. The FT-IR spectrum of FS6 nanoparticles was similar with that of the FS nanoparticles except one new peak at around 1,370 cm $^{-1}$, which was marked by a black line in Fig. 3. According to the previous studies, these new peaks were associated with C–N stretching [22], which was coming from Rhodamine 6G molecules. But because of the confinement effects of SiO_2 shell which hindered most of the stretching and vibrational modes of the dye molecules, the other peaks of Rhodamine 6G are absent in Fig. 3 [10]. So the entrapment of organic dye in the silica shell should be further confirmed by more experimental evidences.

The emission spectra of FS62 and FS6 nanoparticles prepared by different volume of HTMOS were investigated and the results are shown in Fig. 4. As observed, the PL intensity of FS62 nanoparticles was very weak (line a), which demonstrated little Rhodamine 6G molecules were entrapped in the silica matrix. Lines b, c, and d showed the emission peaks of FS6 nanoparticles prepared by 10, 20, and 30 μL of HTMOS, respectively. They all showed intensive emission peaks at 560 nm when excited at 520 nm. Their high PL intensity suggested the organic dye molecules can be entrapped in the silica matrix successfully by the hydrolysis of HTMOS. Furthermore, the maximum intensity of lines b, c, and d in Fig. 4 was increased in turn. This phenomenon indicated that the amount of organic dye doped in the silica shell was increased with the volume of HTMOS increasing [18]. So this data sustained the assumption that the driving force for the entrapment of organic dye molecules was the hydrophobic interaction between organic dye and HTMOS molecules. Furthermore, the PL spectrum of the final sample further confirmed the entrapment of organic dye in the final samples.

The dye leakage behavior of FS6 nanoparticles in aqueous solution was also investigated. Before every measurement, the sample was washed with water and then resuspended in water to the original volume. As shown in Fig. 5, the PL

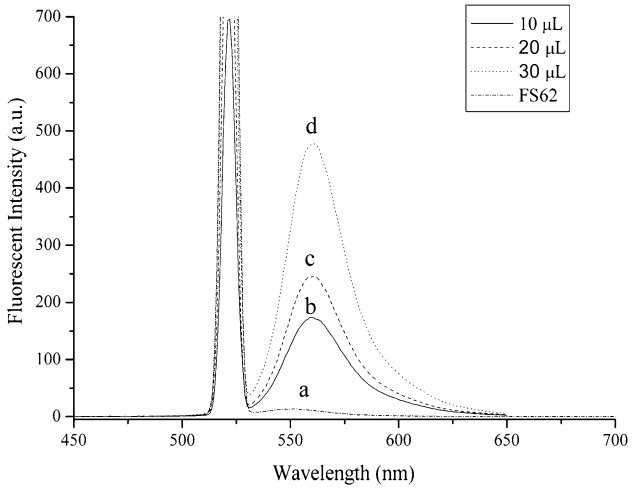

Fig. 4 PL spectra of **a** FS62 nanoparticles and FS6 nanoparticles prepared by different volume of HTMOS, **b** 10 μL, **c** 20 μL, and **d** 30 μL; Ex = 520 nm, Em = 560 nm

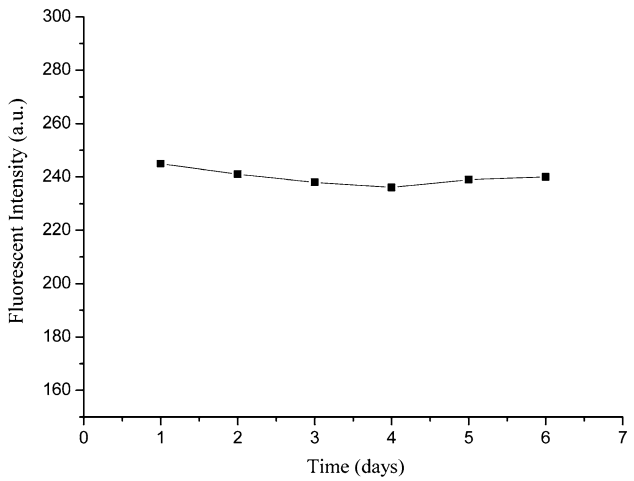

Fig. 5 Fluorescence intensity variation of FS6 nanoparticles immersed in water for 6 days

intensity of the particles measured everyday showed no significant differences in 6 days. It indicated most of the dye molecules were trapped within the nanoparticles and the optical property of the final samples was stable [18].

Figure 6 shows the fluorescence microscopic images of the FS6 nanoparticles. It clearly showed the final particles were bright green dots. On the one hand, the particles were presented as bright dots which indicated the final samples were fluorescent. On the other hand, their green color was in agreement with the PL spectra because their emission wavelength was 560 nm.

Figure 7 shows the magnetization hysteresis loops of the final samples measured at room temperature. The FS6 nanoparticles were superparamagnetic as evidenced by the zero coercivity [23]. It is well known that iron oxide nanoparticles

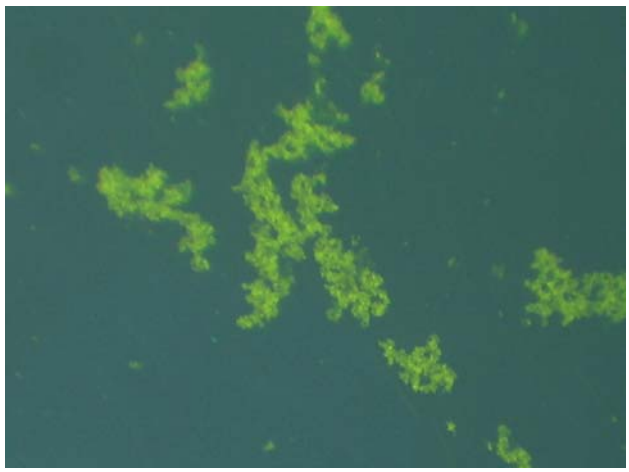

Fig. 6 Confocal fluorescence image of the final FS6 nanoparticles

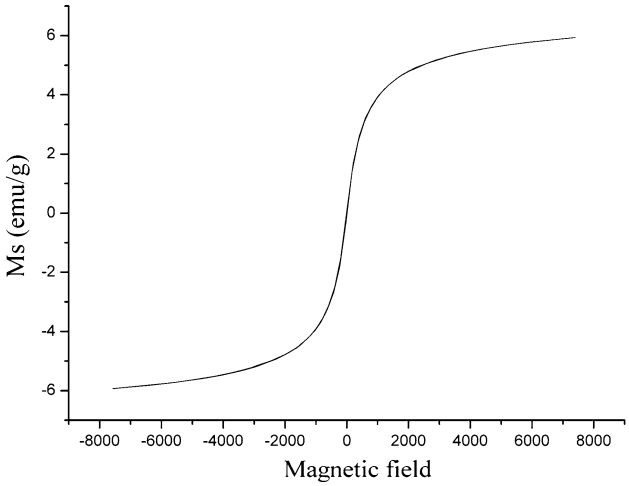

Fig. 7 Magnetization hysteresis loops measured at room temperature for the final FS6 samples

smaller than 20 nm are usually superparamagnetic at room temperature [24]. The mean size of the prepared iron oxide nanoparticles was about 10 nm, so our measurements were in agreement with this view. The saturation magnetization (Ms) of the final samples was about 6 emu/g.

Conclusions

In summary, a new method for preparing iron oxide nanoparticles coated with organic dye-doped silica shell was developed. The preparation procedure was carried out in a bulk aqueous/isopropyl alcohol system at room temperature, which make it environmental friendly and low cost. In addition, the preparation procedure was relatively facile. The characterization results by XRD, TEM, FT-IR, VSM, PL spectra, and Confocal fluorescence microscopy indicated that the final nanoparticles possessed magnetic

and fluorescent properties simultaneously. So this new method was efficient in preparing organic dye-doped silica shell-coated iron oxide nanoparticles. In addition, we predict that this method can be applied to synthesis other fluorescent-magnetic nanoparticles.

Acknowledgments The project was supported by the Open Subject Foundation of Key Laboratory for Magnetism and Magnetic Materials of MOE, Lanzhou University. We also kindly acknowledge the National Science Foundation of China (No. 20875040) for supporting this work.

References

1. D.B. Tada, L.L.R. Vono, E.L. Duarte, R. Itri, P.K. Kiyohara, M.S. Baptista, L.M. Rossi, Langmuir **23**, 8194 (2007). doi:10.1021/la700883y
2. J.H. Lee, Y.W. Jun, S.I. Yeon, J.S. Shin, J. Cheon, Angew. Chem. Int. Ed. **45**, 8160 (2006). doi:10.1002/anie.200603052
3. C.W. Lu, Y. Hung, J.K. Hsiao, M. Yao, T.H. Chung, Y.S. Lin, S.H. Wu, S.C. Hsu, H.M. Liu, C.Y. Mou, C.S. Yang, D.M. Huang, Y.C. Chen, Nano Lett. **7**, 149 (2007). doi:10.1021/nl0624263
4. D.L. Ma, Z.J. Jakubek, B. Simard, J. Nanosci. Nanotechnol. **7**, 1 (2007)
5. D.L. Ma, J.W. Guan, F. Normandin, S. De'nomme'e, G. Enright, T. Veres, B. Simard, Chem. Mater. **18**, 1920 (2006). doi:10.1021/cm052067x
6. E.J. Bergey, L. Levy, X.P. Wang, L.J. Krebs, M. Lal, K.S. Kim, S. Pakatchi, C. Liebow, P.N. Prasad, Biomed. Microdevices **4**, 293 (2002). doi:10.1023/A:1020906307053
7. S.A. Corr, Y.P. Rakovich, Y.K. Gun'ko, Nanoscale Res. Lett. **3**, 87 (2008). doi:10.1007/s11671-008-9122-8
8. H.M. Liu, S.H. Wu, C.W. Lu, M. Yao, J.K. Hsiao, Y. Hung, Y.S. Lin, C.Y. Mou, C.S. Yang, D.M. Huang, Y.C. Chen, Small **4**, 619 (2008). doi:10.1002/smll.200700493
9. A.T. Heitsch, D.K. Smith, R.N. Patel, D. Ress, B.A. Korgel, J. Solid State Chem. **181**, 1590 (2008). doi:10.1016/j.jssc.2008.05.002
10. C.L. Ren, J.H. Li, X.G. Chen, Z.D. Hu, D.S. Xue, Nanotechnology **18**, 345604 (2007)
11. Q.A. Pankhurst, J. Connolly, S.K. Jones, J. Dobson, J. Phys. D.: Appl. Phys. **36**, R167 (2003)
12. A. Bjornerud, L. Johansson, NMR Biomed. **17**, 465 (2004)
13. K. Tanaka, A. Ito, T. Kobayashi, T. Kawamura, S. Shimada, K. Matsumoto, T. Saida, H. Honda, Int. J. Cancer **116**, 624 (2005). doi:10.1002/ijc.21061
14. I.J. Bruce, T. Sen, Langmuir **21**, 7029 (2005). doi:10.1021/la050553t
15. S. Santra, P. Zhang, K.M. Wang, R. Tapec, W.H. Tan, Anal. Chem. **73**, 4988 (2001). doi:10.1021/ac010406+
16. X. He, J. Duan, K. Wang, W. Tan, X. Lin, C. He, J. Nanosci. Nanotechnol. **4**, 585 (2004). doi:10.1166/jnn.2004.011
17. L. Wang, C.Y. Yang, W.H. Tan, Nano Lett. **5**, 37 (2005). doi:10.1021/nl048417g
18. R. Tapec, X.J. Zhao, W. Tan, J. Nanosci. Nanotechnol. **2**, 405 (2002). doi:10.1166/jnn.2002.114
19. T. Deng, J.S. Li, J.H. Jiang, G.L. Shen, R.Q. Yu, Adv. Funct. Mater. **16**, 2147 (2006). doi:10.1002/adfm.200600149
20. M.F. Casula, Y.W. Jun, D.J. Zaziski, E.M. Chan, A. Corrias, A.P. Alivisatos, J. Am. Chem. Soc. **128**, 1675 (2006). doi:10.1021/ja056139x
21. J. Giri, S.G. Thakurta, J. Bellare, A.K. Nigam, D. Bahadur, J. Magn. Magn. Mater. **293**, 62 (2005). doi:10.1016/j.jmmm.2005.01.044
22. A. Barranco, F. Aparicio, A. Yanguas-Gil, P. Groening, J. Cotrino, A.R. González-Elipe, Chem. Vap. Depos. **13**, 319 (2007). doi:10.1002/cvde.200606552
23. Y. Sahoo, A. Goodarzi, M.T. Swihart, T.Y. Ohulchanskyy, N. Kaur, E.P. Furlani, P.N. Prasad, J. Phys. Chem. B **109**, 3879 (2005). doi:10.1021/jp045402y
24. Y. Lee, J. Lee, C. Bae, J. Park, H. Noh, J. Park, T. Hyeon, Adv. Funct. Mater. **15**, 503 (2005). doi:10.1002/adfm.200400187